Confocal spectroscopy of InGaN LED structures

D Dobrovolskas, J Mickevičius, E Kuokštis, G Tamulaitis, M Shur, M Shatalov, J Yang, R Gaska

Confocal spectroscopy of InGaN LED structures

D Dobrovolskas[1], J Mickevičius[1], E Kuokštis[1], G Tamulaitis[1], M Shur[2], M Shatalov[3], J Yang[3], and R Gaska[3]

[1] Semiconductor Physics Department and Institute of Applied Research, Vilnius University, Saulėtekio 9-III, LT-10222 Vilnius, Lithuania

[2] Department of Electrical, Computer, and Systems Engineering, and Center of Integrated Electronics, Rensselaer Polytechnic Institute, 110 Eighth Street, Troy, New York 12180

[3] Sensor Electronic Technology, Inc., 1195 Atlas Rd., Columbia, SC, U.S.A.

E-mail: darius.dobrovolskas@ff.stud.vu.lt

Photoluminescence of InGaN structures for green light emitting diodes with multiple quantum wells as an active medium was studied with spatial and spectral resolution using confocal microscopy. Bright spots of ~200 nm in diameter were observed. Emission from these bright areas was up to 8 times more intense than from the rest of the sample surface and the band peak position in these areas was blueshifted in respect to the band position in the background surface of lower photoluminescence intensity. The data on emission properties in bright and dark areas and the dependence of these properties on the excitation power density are interpreted by assuming inhomogeneous distribution of defects acting as nonradiative recombination centers.

1. Introduction

Localization and inhomogeneous spatial distribution of nonequilibrium carriers (excitons) in InGaN in blue and white light emitting diodes (LEDs) and blue laser diodes play a crucial role in the light emission of InGaN epilayers and heterostructures [1] but peculiarities of these processes are still not fully understood.

Cathodoluminescence (CL) [2, 3, 4, 5], μ-PL [6, 7, 8], confocal spectroscopy [9, 10, 11], and scanning near field optical microscopy (SNOM) [16, 12, 13, 14] all reveal inhomogeneous photoluminescence intensity distribution in InGaN epilayers and QWs. Many publications [15, 16, 17, 18] point out to the

well width fluctuations as the main origin of inhomogeneous spatial PL distribution in InGaN QWs, and dislocations are claimed to have a significant effect on the local emission efficiency [14, 19]. Localization of excitons on a nanometer scale might be also caused by the localization of the hole wave functions around indium in randomly formed In-Ga-In chains, as was theoretically predicted for cubic InGaN [20].

In InGaN quantum wells (QWs), optical transitions and carrier dynamics are affected by the quantum-confined Stark effect (QCSE) due to the built-in electric field, which can be screened by nonequilibrium carriers [11, 21], and by filling-in of the localized states that often have a similar effect on the InGaN QW characteristics.

The present paper reports on the study of spatial distribution of photoluminescence (PL) in LED structures with InGaN multiple quantum wells (MQWs) as an active region. PL spectroscopy in the confocal mode was employed and revealed unusual features of the inhomogeneous PL spatial distribution. For our sample, the strongly pronounced PL features cannot be interpreted as caused by localization and field-induced effects.

2. Experimental

The green LED structure under study was grown on the *c*-plane sapphire by metal-organic chemical vapor deposition. Trimethyl indium (TMI), trimethyl gallium (TMGa) and ammonia (NH_3) were used as In, Ga and N sources, respectively. The structure consisted of a 0.3 μm thick AlN buffer layer, 3 μm thick Si-doped *n*-GaN layer, InGaN compliance layer, 5-period InGaN/GaN MQW active layer, 20 nm thick *p*-AlGaN electron block, and 0.2 μm thick *p*-type contact layer. The active layer contained 2 nm wide $In_{0.27}Ga_{0.73}N$ wells and 5 nm wide GaN barriers.

The PL intensity mapping and study of spatial variations in PL spectra on submicrometer scale have been performed using *WITec* confocal microscope *Alpha* 300 S. Objective with numerical aperture NA = 0.9 was used ensuring in-plane spatial resolution of ~200 nm. For spectral resolution, the microscope was coupled by an optical fiber with a *Cromex* spectrometer followed by a thermoelectrically cooled CCD camera. A CW He-Cd laser emitting at 442 nm was employed for the excitation. All the experiments have been carried out at room temperature.

Excitation power density dependence of the relative quantum efficiency of spatially-integrated PL in a wide dynamic range have been carried out under quasi-steady-state excitation by the third harmonic of Q-switched YAG:Nd laser radiation (3.49 eV).

3. Results

The mapping images of spectrally integrated PL intensity are presented in figure 1(*a*). The figure reveals a strongly inhomogeneous spatial distribution of emission intensity in the MQW plane: regions of stronger emission are evident on the field of lower emission intensity. The bright spots in the mapping image typically have a round shape of ~200 nm in diameter (close to the spatial resolution of the confocal microscope used). The PL intensity in the bright spots exceeds the background intensity by a factor of up to 8.

The spectral PL distribution in the MQW plane was studied by comparing the emission spectra in small spots (50×50 nm, 5×5 pixels) picked up from the regions of low and high emission intensity (dark and bright areas, as referred to further in this paper). Several of these PL spectra are presented for bright and dark areas in figure 1(*b*) and (*c*), respectively. The spots, from which the corresponding spectra were acquired, are marked and labeled in the mapping images [figure 1(*a*)]. A considerable scattering in intensities and peak wavelengths of the PL bands acquired from different spots in the bright and dark areas is quite evident. The resulting FWHM of the spatially-integrated PL band (measured at high excitation intensities when a single band prevails) is 38 nm in bright and 51 nm in dark areas.

The spatially-integrated dark area band peak is redshifted by 10 nm in respect to the band position in the bright areas. The comparison of the PL bands recorded from different spots shows that this redshift and broadening of the spatially-integrated PL band in the dark areas is caused by a lower intensity of PL emitted from spots corresponding to shorter wavelengths, while the emission intensities in the long wavelength region are similar in the dark and bright areas (see figure 2).

To gain more data on possible mechanisms of the inhomogeneous PL intensity distribution, we studied the PL properties of our sample at different nonequilibrium carrier densities. Figure 3 presents the PL spectra measured in a dark area at different excitation power densities. The spectrum is basically dominated by the single band, which is peaked at ~500 nm and shows a considerable band

shift with increasing excitation. In addition to the prevailing band, another PL band [peaked at considerably longer wavelengths (~560 nm)] was observed in the dark areas, but its intensity saturated with increasing excitation. This PL band probably involves defect-related states. No long-wavelength band was observed in the bright areas.

The excitation power density dependences of the peak position of the main PL band for the bright and dark areas are compared in figure 4(*a*). The band peak in the dark areas gradually blueshifts by ~25 nm when the excitation power density is increased from 4×10^{-3} to 2.4 MW/cm^2. A striking feature is that the band peak in the bright areas at low excitation power densities is at a shorter wavelength than that in the dark areas. With increasing excitation intensity, the PL band in bright areas first blueshifts slower than that in dark areas but the shift rate becomes similar in both areas at high excitation intensities.

The excitation power density dependences of the spectrally integrated PL intensity in bright and dark areas are presented in figure 4(*b*). The dependence is linear at low excitation, but becomes superlinear at elevated excitation power densities. To study the PL efficiency dependence on excitation power density in a wider dynamic range, experiments have been performed under quasi-steady-state pulsed (pulse duration 4.4 ns) [figure 4(*c*)]. Note that the photon energy in quasi-steady-state pulsed excitation (3.49 eV) was high enough to excite the 5 nm wide barriers, while in CW excitation (photon energy 2.81 eV) only the 2 nm-wide quantum wells were excited. Thus, at the same excitation power density, the expected carrier density under the pulsed excitation is larger than that under selective excitation approximately by a factor of 3. Moreover, the small excess energy of the photoexcited carriers might also diminish the spillover effect, which probably is one of the mechanisms causing the efficiency droop effect [22]. Comparison of figure 4(*b*) and figure 4(*c*) shows that the droop is observed at a higher carrier density than that achieved in our spatially-resolved experiments.

4. Discussion

The PL band shift with increasing excitation intensity in InGaN QWs is usually explained by two effects: gradual population of the lowest localized states and screening of the built-in electric field. Both effects result in a blue shift of the PL band and their contributions are difficult to distinguish.

We calculated the energy levels in quantum well with a built-in electric field by simultaneously solving the stationary Schrödinger equation and the Poisson equation describing the asymmetric space–charge distribution in the well. Using material parameters taken from Ref. [23] and approach suggested in Ref. [24] results in the built-in field at GaN/$In_{0.27}Ga_{0.73}N$ of 3.4 MV/cm. Such a field shifts the energy of the lowest optical transition by ~200 meV. The built-in field of 1.5 MV/cm, which is a typical low-bound value estimated for similar GaN/InGaN interfaces [25], results in a shift of ~60 meV. Carrier densities sufficient to cause a significant blue shift of the lowest optical transition due to screening of the built-in field are lower in wider QWs. In the 2 nm-wide well under study, a blue shift of 10% from the entire QCSE shift occurs at densities of ~2×10^{12} cm^{-2}. The estimation of the carrier density in our PL experiments is obscured by uncertainty in the carrier lifetime, which locally depends on the carrier localization depth and on the carrier density. Assuming the lifetime to be 1 ns, the excitation power densities in our experiments (from 4 kW/cm^2 to 2.4 MW/cm^2) correspond to the carrier densities ranging from 2×10^{10} cm^{-2} to 10^{13} cm^{-2}. Thus, the faster blue shift of the PL band at the highest excitation power densities in our experiments should be influenced by the screening effect but the lowest excitation intensities used hardly influence screening. This conclusion is supported by the excitation power density dependence of the PL intensity [see figure 4(*b*)], which is linear at a low excitation but becomes superlinear at the excitation power densities exceeding approximately 0.1 MW/cm^2. There is no return of the linear dependence, which is expected after the built-in field is completely screened. This might be an indication that the built-in field is not completely screened even at the highest excitation power densities used in our experiments. On the other hand, the superlinear growth of PL intensity at increasing excitation power density might also be expected due to the saturation of nonradiative recombination centers.

Localization and inhomogeneous spatial carrier distribution due to the fluctuations in indium content and/or well width definitely plays an important role in the samples under study. It is usually assumed that the deeper carrier (exciton) localization (corresponding to a lower energy of the photon emitted via radiative recombination in the localized states) results in a higher PL intensity due to decreased probabilities of carrier hopping and reaching nonradiative recombination centers. Thus, the inhomogeneous PL intensity distribution could be explained by inhomogeneous distribution of deep

localized states. Contrary to this assumption, the PL peak position in the bright areas of the sample under study is higher in energy than in the dark areas.

The difference in $In_xGa_{1-x}N$ content with $x \approx 0.27$ corresponding to the PL band shift observed (~10 nm) would be rather small (of the order of $\Delta x = 0.01$) and hardly could cause the observed increase in PL intensity by a factor of 8 due to possibly higher structural quality in the areas with lower In content.

The bright spots could have been interpreted as regions with narrower well width, where the blue shift of the PL band is stronger and the PL intensity is higher due to stronger overlap of the electron and hole wavefunctions. Though qualitatively consistent with experimental results, this effect is expected to be considerably weaker than observed. At low carrier density, the square of the wavefunction overlap for 1.75 nm wide well exceeds that for 2.25 nm well by a factor of two. This difference will be even lower due to stronger screening in the thicker regions, where a higher carrier density should be expected. Such difference is insufficient to explain the observed intensity difference of up to the factor of 8.

The lower PL intensity in areas where emission occurs at longer wavelength might have been explained by an inhomogeneous spatial distribution of the built-in field: a higher field causes a larger PL band redshift due to QCSE and, hence, a smaller overlap of the electron and hole wavefunctions and, consequently, a smaller rate of radiative recombination and a lower emission intensity. However, according to our calculations discussed above, this effect cannot explain such a big difference in the observed PL intensity in the bright and dark areas. The difference of ~25 nm observed for PL band peak positions in bright and dark areas at low excitation power density [see figure 4(*a*)] corresponds to variation of the built-in field by ~30%. The built-in field of 3.4 MV/cm causes a decrease of the squared electron and hole wavefunction overlap in a 2 nm QW down to 25% of the value for a rectangle QW (with zero built-in field). Variation of the field by 30% results in 1.5 times change, in the PL intensity due to the overlap change, which is much smaller than the observed factor of 8.

We suggest that the inhomogeneous PL intensity distribution observed in the structure under study can be explained by an inhomogeneous distribution of nonradiative recombination centers, as previously reported in [26]. The probability of nonradiative recombination is higher for the carriers (excitons) occupying the states with smaller localization energy. These excitons, which are responsible

for the short-wavelength side of the PL band, have a higher probability to reach nonradiative recombination centers by hopping. Thus, the nonradiative recombination suppresses emission mainly on the high energy side of the PL band resulting in a redshift. The higher is the density of nonradiative recombination centers, the stronger is the redshift. Thus, the PL band in the dark areas is at longer wavelength than that in the bright ones. This interpretation is strongly supported by the data presented in figure 2. As seen, the intensity is equal both in bright and dark areas at the long-wavelength tail of the PL band, but the intensity in bright areas is progressively higher at the shorter wavelengths.

As the carrier density increases, more localized states get occupied. This effect results in a blue shift, which compensates the red shift caused by the nonradiative recombination centers. The blue shift due to the state filling is stronger in the spectral region corresponding to the tail of the density of the localized states and becomes less pronounced in the spectral region corresponding to a higher density of states. The results presented in figure 4(*a*) are consistent with this interpretation: the PL band blue shift at increasing excitation power density is more pronounced in the dark areas. As discussed above, the overall blue shift, which is observed in the bright areas, should be influenced by screening of the built-in field.

The conclusion that the inhomogeneous PL spatial distribution is strongly affected by an inhomogeneous distribution of the nonradiative recombination centers is indirectly supported by observation that the additional long-wavelength emission band is present in the dark but not in the bright areas. As shown in Ref. [27] for GaN, the densities of nonradiative recombination centers and the centers of radiative defect-related recombination (causing yellow luminescence) are correlated. Provided that a similar conclusion is valid also for InGaN, the presence of the long-wavelength PL band in dark areas is an indication that these areas contain also a higher density of nonradiative recombination centers. The unusual PL characteristics and their dynamics under increasing excitation power density are consistent with the assumption that this sample has inhomogeneous distribution of nonradiative recombination centers. This feature can be favorable for higher emission efficiency. In the areas with a lower density of nonradiative recombination centers, the carrier density is higher and screens the built-in field more effectively.

Spectrally-integrated PL intensity dependence on carrier density [see figure 4(*b*)] is the same in bright and dark areas but a higher excitation power density is necessary to reach the same carrier density in the dark areas due to a higher density of nonradiative recombination centers.

The origin of inhomogeneous distribution of nonradiative recombination centers is unclear. It is worth noting, however, that the structure under study contains 5 QWs. The spatial resolution in the Z direction (perpendicular to the layers) is 0.75 μm, i.e. includes all the QWs. Hence, the bright areas vertically coincide within ~200 nm in all five QWs. Otherwise, the image would be washed out, and no distinct bright areas of ~200 nm in diameter would be observed. Such a vertical alignment implies possible involvement of dislocations propagating vertically though the QWs. At dislocation density of 10^9 cm^{-2}, the 2×2 μm sample area depicted in figure 1(*a*) should contain 40 dislocations on average. It can be expected that these dislocations concentrate in the dark areas and are absent in the bright areas. To prove the model of inhomogeneous distribution of nonradiative recombination centers and to reveal the origin of the centers, results on microstructural analysis could be helpful and will be published elsewhere.

5. Conclusions

Confocal microscopy reveals spots of a more intense photoluminescence (~200 nm in diameter) in green LED structures with $In_{0.27}Ga_{0.73}N$ MQWs as an active region. The spectral features in the dark and bright areas and dynamics of the photoluminescence characteristics under increasing excitation power density point out to an inhomogeneous distribution of nonradiative recombination centers affecting the carrier density distribution and screening of the built-in field in the QWs leading to nonuniform emission intensity.

Acknowledgments

This work was supported by the National Science Foundation (NSF) Smart Lighting Engineering Research Center (# EEC-0812056) and by the National Science Foundation (NSF) I/UCRC “Connection One”. The work at Vilnius University was partially supported by the Lithuanian Science and Study Foundation (Grant No. T-74/09). Authors would also like to acknowledge partial support

from US ARMY RDECOM SBIR Phase I contract (W911NF-07-C-0072) monitored by Dr. Marc Ulrich (ARO). Authors would like to thank Vytautas Liuolia for his contribution to calculations.

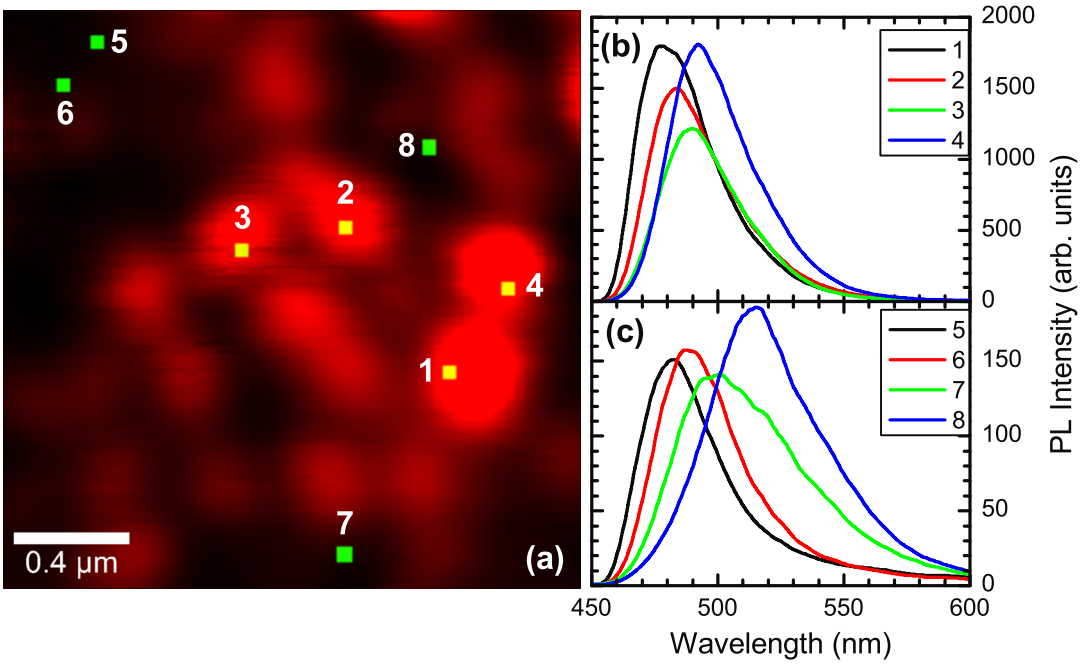

Figure 1. Typical PL intensity mapping (2×2 μm) image of InGaN-based LED structure (a) and several PL spectra taken from spots indicated on the map in bright (b) and dark (c) areas.

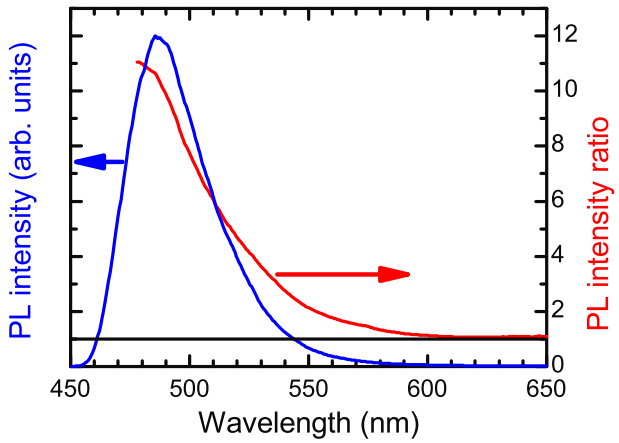

Figure 2. Spatially-integrated PL spectrum in bright areas (blue curve) and spectral distribution of ratio of PL intensity spatially integrated in bright and dark areas (red curve).

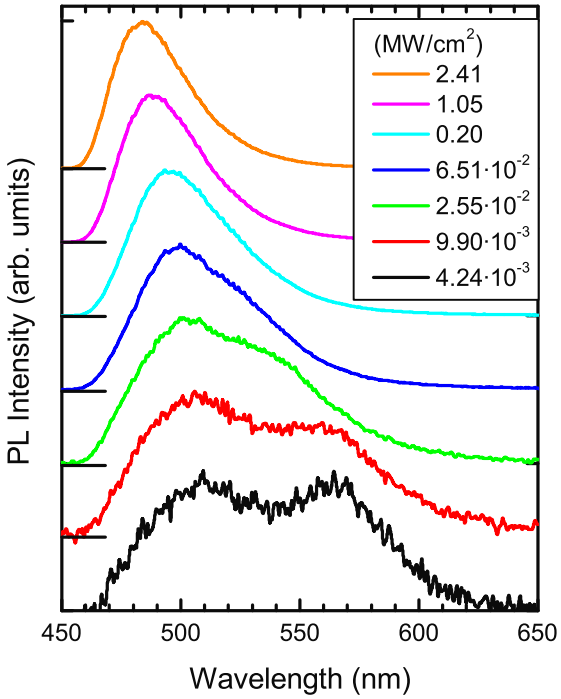

Figure 3. Excitation power density dependence of PL spectrum in dark area. The spectra are normalized and shifted along Y axis for clarity.

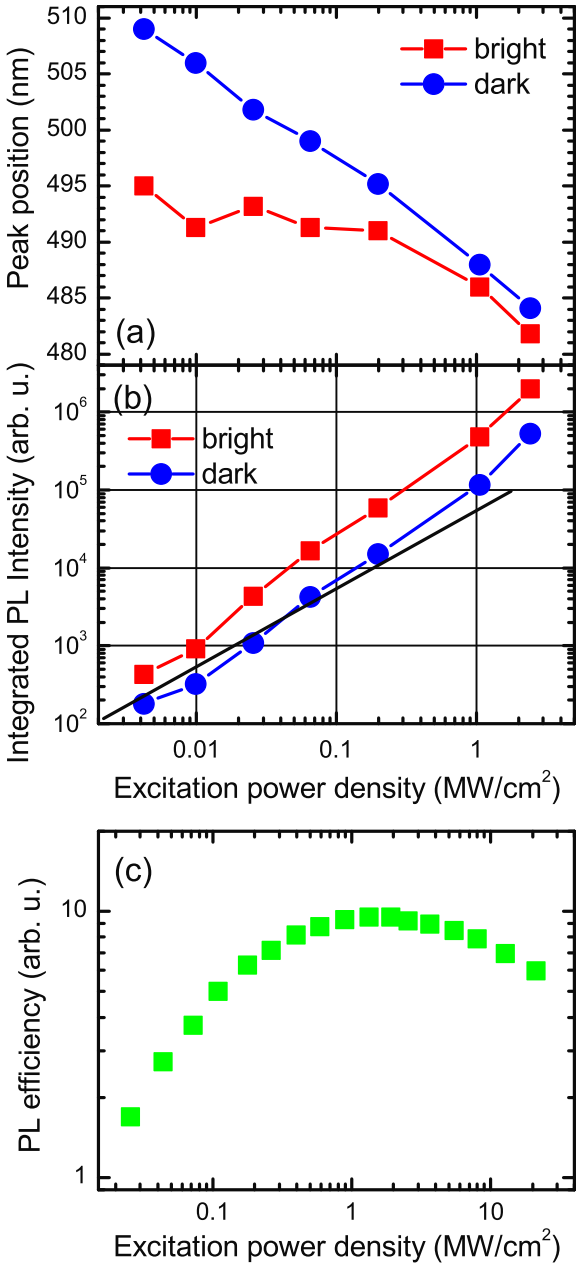

Figure 4. PL band peak position (a) and spectrally integrated PL intensity (b) in dark and bright areas as a function of excitation power density under selective CW well excitation and spatially-integrated PL efficiency dependence on excitation power density under pulsed excitation above barrier band gap (c). Solid line in (b) shows linear PL intensity dependence.

References

[1] Chichibu S F, Uedono A, Onuma T, Haskell B, Chakraborty A, Koyama T, Fini P T, Keller S, DenBaars S P, Speck J S, Mishra U K, Nakamura S, Yamaguchi S, Kamiyama S, Amano H, Akasaki I, Han J, and Sota T 2006 *Nature Materials* **5** 810.

[2] Chichibu S, Wada K, and Nakamura S 1997 *Appl. Phys.* Lett. **71** 2346.

[3] Bertram F, Srinivasan S, Geng L, Ponce F A, Riemann T, Christen J, Tanaka S, Omiya H, and Nakagawa Y 2001 *Phys. Stat. Sol*. B **228** 35.

[4] Cherns D, Henley S J, and Ponce F A 2001 *Appl. Phys. Lett.* **78** 2691.

[5] Brooksby J C, Mei J, and Ponce F A 2007 *Appl. Phys. Lett.* **90** 231901.

[6] Gotoh H, Akasaka T, Tawara T, Kobayashi Y, Makimoto T, and Nakano H 2006 *Sol. Stat. Comm.* **138** 590.

[7] Oh E, Park H, Sone C, Nam O, Park Y, and Kim T 2000 *Sol. Stat. Comm.* **113** 461.

[8] Ko T S, Lu T C, Wang T C, Chen J R, Gao R C, Lo M H, Kuo H C, Wang S C, and Shen J L 2008 *J. Appl. Phys.* **104** 093106.

[9] O'Donnell K P, Cowan C T, Pereira S, Bangura A, Young C, White M E, and Tobin M J 1999 *Phys. Stat. Sol.* B **216** 157.

[10] Vierheilig C, Braun H, Schwarz U T, Wegscheider W, Baur E, Strauß U, and Härle V 2007 *Phys. Stat. Sol.* C **4** 2362.

[11] Okamoto K, Kaneta A, Kawakami Y, Fujita S, Choi J, Terazima M, and Mukai T 2005 *J. Appl. Phys.* **98** 064503.

[12] Hitzel F, Hangleiter A, Bader S, Lugauer H–J, and Härle V 2001 *Phys. Stat. Sol.* B. **228** 407.

[13] Kaneta A, Okamoto K, Kawakami Y, Fujita S, Marutsuki G, Narukawa Y, and Mukai T 2002 *Appl. Phys. Lett.* **81** 4353.

[14] Kaneta A, Funato M, and Kawakami Y 2008 *Phys. Rev.* B **78** 125317.

[15] Narayan J, Wang H, Jinlin Ye, Hon S–J, Fox K, Chen J C, Choi H K, and Fan J C C 2002 *Appl. Phys. Lett.* **81** 841.

[16] Graham D M, Soltani–Vala A, Dawson P, Godfrey M J, Smeeton T M, Barnard J S, Kappers M J, Humpreys C J, and Thrush E J 2005 *J. Appl. Phys.* **97** 103508.

[17] Kwon S Y, Kim H J, Yoon E, Jang Y, Yee K–J, Lee D, Park S–H, Park D–Y, Cheong H, Rol F, and Dang L S 2008 *J. Appl. Phys.* **103** 063509.

[18] Sonderegger S, Feltin E, Merano M, Crottini A, Carlin J F, Sachot R, Deveaud B, Grandjean N, and Ganiere J D 2006 *Appl. Phys. Lett.* **89** 232109.

[19] Hangleiter A, Hitzel F, Netzel C, Fuhrmann D, Rossow U, Ade G, and Hinze P 2005 *Phys. Rev. Lett.* **95** 127402.

[20] Bellaiche L, Matilla T, Wang L–W, Wei S–H, and Zunger A 1999 *Appl. Phys. Lett.* **74** 1842.

[21] Riblet P, Hirayama H, Kinoshita A, Hirata A, Sugano T, Aoyagi Y 1999 *Appl. Phys. Lett*, **75** 2241.

[22] Ozgur U, Liu H, Xing L, Xianfeng N, and Morkoc H 2010 *Proc. IEEE* **98** 1180.

[23] Vurgaftman I and Meyer J R 2003 *J. Appl. Phys.* **94** 3675.

[24] Fiorentini V, Bernardini F, Della Sala F, Di Carlo A, and Lugli P 1999 *Phys. Rev. B.* **60** 8849.

[25] Dialynas G E, Deligeorgis G, Zervos M, and Pelekanos N T 2008 *J. Appl. Phys.* **104** 113101.

[26] Tamulaitis G, Mickevičius J, Dobrovolskas D, Kuokštis E, Shur M, Shatalov M, Yang J, and Gaska R 2010 *Phys. Status Solidi C* **7** 1869.

[27] Mickevičius J, Aleksiejūnas R, Shur M S, Sakalauskas S, Tamulaitis G, Fareed Q, and Gaska R 2005 *Appl. Phys. Lett.* **86** 041910.